

5.5. Theory of Gratings

Gratings are periodic structures that, when illuminated by a coherent light beam, scatter light into diffraction orders. Some gratings are thin, so that the light transmitted through the grating or reflected from it is described by a simple multiplication of the incident field and the grating structure. Other gratings are thicker and require a more complete analysis.

Diffraction from thin gratings can be explained in two ways. Section 5.5.1 uses the geometrical technique that was developed for a Fresnel lens in order to describe diffraction from a grating, and Section 5.5.2 uses a mathematical development that assumes the observation plane is in the Fraunhofer region of the illuminated grating. For both techniques, gratings are assumed to be thin phase or amplitude objects, and the period of the grating is large relative to illumination wavelength. Thin gratings have useful characteristics with respect to analyzing sources with multiple wavelengths. These properties are analyzed in Section 5.5.3.

Diffraction from thick gratings is described by Bragg diffraction, which is explained in Section 5.5.4. Thick gratings form the basis for operation of acousto-optic transducers, volume holography and other useful techniques.

5.5.1 Geometric OPD theory for thin gratings

Consider a screen illuminated with a plane wave that contains an array of N regularly-spaced narrow slits within aperture diameter $2a$, as shown in Fig. 5.72. The observation plane is in the Fraunhofer region of the aperture. A small section of the aperture, containing one period of the array, is shown in Fig. 5.73. The \mathbf{k}_S vector of the incident plane wave is in the plane of the drawing. Between any two adjacent slits, total OPD to the observation point is the summation of OPD_S and OPD_0 . When the total OPD between light arriving at the observation point from adjacent slits is equal to $m\lambda$, where m is an integer, constructive interference occurs, and maximum irradiance is observed. A bright spot occurs wherever

$$n_S \sin \theta_S + n_0 \sin \theta_0 = \frac{m\lambda}{d} \quad , \quad (5.166)$$

where n_S and n_0 are refractive indices on illumination and observation sides of the aperture, respectively. Slits are equally spaced, so OPD between every pair of slits is the same when Eq. (5.166) is satisfied. When the number of illuminated slits N is large, OPD differences along the array produce quickly decreasing irradiance as the observation angle θ_0 changes away from this condition. Bright spots are separated by relatively low irradiance. (This effect is described with respect to Fraunhofer diffraction from multiple slits in Section 5.4.6.) Equation (5.166) is often written with $\theta_0 = \theta_m$, where

$$n_S \sin \theta_S + n_0 \sin \theta_m = \frac{m\lambda}{d} \quad . \quad (5.167)$$

The slit array is called a *grating*, and Eq. (5.167) is called the *grating equation*. Bright spots in the observation plane are called *diffraction orders*, and they are labeled with respect to the corresponding number of wavelengths of OPD, as shown in Fig. 5.74.

A modification of Eq. (5.167) is required if the incident plane wave \mathbf{k}_S vector is not in the plane perpendicular to the grating lines. We define vector $\hat{\mathbf{g}}$ in a direction aligned with the grating modulation. (For the example shown in Fig. 5.72, \mathbf{k}_S is in the yz plane and $\hat{\mathbf{g}}$ is in the $\hat{\mathbf{y}}$ direction.) Values for OPD_S and OPD_0 are given by

$$\text{OPD}_S = n_S d \hat{\mathbf{k}}_S \cdot \hat{\mathbf{g}} \quad , \quad (5.168)$$

with $\hat{\mathbf{k}}_S = \alpha_S \hat{\mathbf{x}} + \beta_S \hat{\mathbf{y}} + \gamma_S \hat{\mathbf{z}}$ and

$$\text{OPD}_0 = n_0 d \hat{\mathbf{k}}_0 \cdot \hat{\mathbf{g}} \quad , \quad (5.169)$$

with $\hat{\mathbf{k}}_0 = \alpha_0 \hat{\mathbf{x}} + \beta_0 \hat{\mathbf{y}} + \gamma_0 \hat{\mathbf{z}}$, respectively. If $\hat{\mathbf{g}}$ is in the $\hat{\mathbf{y}}$ direction,

$$\begin{aligned} \text{OPD} &= n_S d \hat{\mathbf{k}}_S \cdot \hat{\mathbf{y}} + n_0 d \hat{\mathbf{k}}_0 \cdot \hat{\mathbf{y}} \\ &= n_S d \beta_S + n_0 d \beta_0 \quad . \end{aligned} \quad (5.170)$$

For constructive interference into diffraction order m with $\beta_0 = \beta_m$,

$$n_S \beta_S + n_0 \beta_m = \frac{m\lambda}{d} \quad . \quad (5.171)$$

The x -component of the constructive interference is not modified by passing the plane wave through the $\hat{\mathbf{y}}$ -oriented grating, so $\alpha_m = \alpha_S$. Therefore, the z -direction cosine of the diffracted wave is given by

$$\begin{aligned} \gamma_m &= \sqrt{1 - \alpha_S^2 - \beta_m^2} \\ &= \sqrt{1 - \alpha_S^2 - \left(\frac{m\lambda}{n_0 d} - \frac{n_S \beta_S}{n_0} \right)^2} \quad , \end{aligned} \quad (5.172)$$

where Eq. (5.172) was used to find β_m , so the diffraction vector \mathbf{k}_m corresponding to order m is given by

$$\mathbf{k}_m = \frac{2\pi n_0}{\lambda} \left[\alpha_S \hat{\mathbf{x}} + \left(\frac{m\lambda}{n_0 d} - \frac{n_S \beta_S}{n_0} \right) \hat{\mathbf{y}} + \sqrt{1 - \alpha_S^2 - \left(\frac{m\lambda}{n_0 d} - \frac{n_S \beta_S}{n_0} \right)^2} \hat{\mathbf{z}} \right] \quad . \quad (5.173)$$

5.5.2 Fraunhofer diffraction from thin gratings

Mathematical analysis of diffraction from gratings follows from Eq. (5.49). A one-dimensional grating, with modulation along the y_s axis, is defined with transmission $f_d(y_s)$ over the base period d . Transmission of the grating inside a circular aperture is given by

$$t(x_s, y_s) = \left[f_d(y_s) \text{rect}\left(\frac{y_s}{d}\right) * \frac{1}{d} \text{comb}\left(\frac{y_s}{d}\right) \right] \frac{1}{2a} \text{circ}\left(\frac{\sqrt{x_s^2 + y_s^2}}{2a}\right) \quad (5.174)$$

A simple diagram illustrating a square-wave transmission phase grating is shown in Fig. 5.75(a), a square-wave transmission amplitude grating is shown in Fig. 5.75(b), and a reflection grating is illustrated in Fig. 5.75(c). The associated base period functions $f_d(y_s)$ are shown for each grating type.

5.5.2.1 Classical plane-wave illumination

Classical plane-wave illumination is observed when the grating with is illuminated with angles of incidence that are in the plane defined by $\hat{\mathbf{g}}$ and the normal to the surface, like the geometry of Fig. 5.72. With plane-wave illumination given by

$$U_s^-(x_s, y_s) = A \exp\left(j2\pi \frac{\beta_s}{\lambda} y_s\right) \quad (5.175)$$

the Fraunhofer diffraction pattern is

$$\begin{aligned} U_0(x_0, y_0) &= -\frac{j e^{jkz_0}}{\lambda z_0} \exp\left[j \frac{k}{2z_0} (x_0^2 + y_0^2)\right] \mathbf{F}_{\eta=\frac{y_0}{\lambda z_0}} \mathbf{F}_{\xi=\frac{x_0}{\lambda z_0}} \left[U_s^+(x_s, y_s) \right] \\ &= -\frac{j e^{jkz_0}}{\lambda z_0} \exp\left[j \frac{k}{2z_0} (x_0^2 + y_0^2)\right] \\ &\quad \times \mathbf{F}_{\eta=\frac{y_0}{\lambda z_0}} \mathbf{F}_{\xi=\frac{x_0}{\lambda z_0}} \left\{ A \exp\left(j2\pi \frac{\beta_s}{\lambda} y_s\right) \left[f_d(y_s) \text{rect}\left(\frac{y_s}{d}\right) * \frac{1}{d} \text{comb}\left(\frac{y_s}{d}\right) \right] \text{circ}\left(\frac{\sqrt{x_s^2 + y_s^2}}{2a}\right) \right\}. \end{aligned} \quad (5.176)$$

The solution to Eq. (5.176) is

$$\begin{aligned}
U_0(x_0, y_0) &= -\frac{Aje^{jkz_0}}{\lambda z_0} e^{j\frac{k\rho_0^2}{2z_0}} \left\{ \delta\left(\eta - \frac{\beta_s}{\lambda}\right) * \mathbf{F}_\eta \left[f_d(y_s) \text{rect}\left(\frac{y_s}{d}\right) \right] \frac{1}{d} \sum_{m=-\infty}^{\infty} \delta\left(\eta + \frac{m}{d}\right) \delta(\xi) \right\} \\
&\quad ** \pi a^2 \text{somb}\left(2a\sqrt{\xi^2 + \eta^2}\right) \Big|_{\xi=\frac{x_0}{\lambda z_0}, \eta=\frac{y_0}{\lambda z_0}} \\
&= -\frac{\pi a^2 Aje^{jkz_0}}{\lambda z_0} e^{j\frac{k\rho_0^2}{2z_0}} \sum_{m=-\infty}^{\infty} \mathbf{F}_m \left[f_d(y_s) \frac{1}{d} \text{rect}\left(\frac{y_s}{d}\right) \right] \text{somb}\left(2a\sqrt{\xi^2 + \left(\eta + \frac{m}{d} - \frac{\beta_s}{\lambda}\right)^2}\right) \Big|_{\xi=\frac{x_0}{\lambda z_0}, \eta=\frac{y_0}{\lambda z_0}} \\
&= -\frac{\pi a^2 Aje^{jkz_0}}{\lambda z_0} e^{j\frac{k\rho_0^2}{2z_0}} \sum_{m=-\infty}^{\infty} \mathbf{F}_m \left[f_d(y_s) \frac{1}{d} \text{rect}\left(\frac{y_s}{d}\right) \right] \text{somb}\left(\frac{2a}{\lambda z_0} \sqrt{x_0^2 + \left(y_0 + \frac{m\lambda z_0}{d} - \beta_s z_0\right)^2}\right)
\end{aligned} \tag{5.177}$$

Notice that the diffraction pattern from a grating in a round aperture illuminated by a plane wave is a weighted summation of $\text{somb}()$ functions in the observation plane. The weighting factors are the Fourier transform harmonics of the base period transmission. The diffraction orders are separated along the observation axis by integer multiples of $\lambda z_0/d$. With the small angle approximation $\theta_m \approx y_0/z_0$ and the wavelength scaled appropriately for the refractive index $\lambda' = \lambda/n_0$, these locations are consistent with the grating equation of Eq. (5.167). As the period d decreases, the orders separate in space. Orders are uniformly shifted along the y_0 axis according to the incident angle of the incident plane wave. The size of each order is the Fraunhofer pattern of the aperture without the grating. As the aperture diameter $2a$ increases, the diameter of each order decreases.

If we assume that aperture diameter $2a$ is large compared to period d , individual diffraction orders are well separated on the observation plane. As an approximation to the irradiance, each diffraction order is summed independently, where

$$I_0(x_0, y_0) \approx \left(\frac{\pi a^2 A}{\lambda z_0}\right)^2 \sum_{m=-\infty}^{\infty} \left| \mathbf{F}_m \left[f_d(y_s) \frac{1}{d} \text{rect}\left(\frac{y_s}{d}\right) \right] \right|^2 \text{somb}^2 \left[\frac{2a}{\lambda z_0} \sqrt{x_0^2 + \left(y_0 + \frac{m\lambda z_0}{d} - \beta_s z_0\right)^2} \right]. \tag{5.178}$$

The *absolute diffraction efficiency* E_m^A is the amount of power in each diffracted order, relative to the total power incident on the grating. For Eq. (5.178), the diffraction efficiency into each order is

$$E_m^A = \left| \mathbf{F}_m \left[f_d(y_s) \frac{1}{d} \text{rect}\left(\frac{y_s}{d}\right) \right] \right|^2 \quad . \quad (5.179)$$

For example, consider a sine wave amplitude grating with

$$f_d(y_s) = \left[a_0 + b_0 \sin(2\pi y_s / d) \right] \quad , \quad (5.180)$$

so

$$\begin{aligned} E_m^A &= \left| \mathbf{F}_m \left\{ \left[a_0 + b_0 \sin(2\pi y_s / d) \right] \frac{1}{d} \text{rect}\left(\frac{y_s}{d}\right) \right\} \right|^2 \\ &= \left| a_0 \text{sinc}(m) + b_0 \frac{\text{sinc}(m-1) - \text{sinc}(m+1)}{4j} \right|^2 \quad . \end{aligned} \quad (5.181)$$

Therefore, $E_0^A = 0.25$ (25%) and $E_{\pm 1}^A = 0.0625$ (6.25%) with $a_0 = b_0 = 1$. No other orders are present in the diffraction pattern. Summation of the absolute diffraction efficiencies is less than one, because the diffraction grating is partially absorbing. The *relative diffraction efficiency* E_m^R can be defined with respect to reflection from or transmission through a smooth surface or, in this case, with respect to the total transmitted power. The reference power must be clearly understood when calculating E_m^R . For E_m^A in Eq. (5.181), relative diffraction efficiencies with respect to the total transmitted power are $E_0^R = 2/3$ and $E_{\pm 1}^R = 1/6$. Figures 5.76 through 5.78 display several typical types of gratings and their efficiencies.

5.5.2.3 Large-angle diffraction from thin gratings

With plane-wave illumination given by

$$\begin{aligned} U_s^-(x_s, y_s) &= A \exp(j\mathbf{k}_s \cdot \mathbf{r}_s) \\ &= A \exp \left[j2\pi \left(\frac{\alpha_s}{\lambda} x_s + \frac{\beta_s}{\lambda} y_s \right) \right] \end{aligned} \quad (5.182)$$

and the assumption of Eq. (5.152), the Fraunhofer diffraction pattern on an observation hemisphere with radius r is

$$\begin{aligned}
U_0(\xi, \eta) &= -\frac{j\gamma e^{jkr}}{\lambda r} \mathbf{F}_{\frac{\beta}{\lambda}=\eta} \mathbf{F}_{\frac{\alpha}{\lambda}=\xi} \left[U_S^+(x_S, y_S) \right] \\
&= -\frac{j\gamma e^{jkr}}{\lambda r} \mathbf{F}_{\frac{\beta}{\lambda}=\eta} \mathbf{F}_{\frac{\alpha}{\lambda}=\xi} \left\{ A \exp \left[j2\pi \left(\frac{\alpha_S}{\lambda} x_S + \frac{\beta_S}{\lambda} y_S \right) \right] \left[f_d(y_S) \text{rect} \left(\frac{y_S}{d} \right) * \frac{1}{d} \text{comb} \left(\frac{y_S}{d} \right) \right] \text{circ} \left(\frac{\sqrt{x_S^2 + y_S^2}}{2a} \right) \right\} \\
&= -\frac{j\gamma A e^{jkr}}{\lambda r} \left\{ \delta \left(\xi - \frac{\alpha_S}{\lambda}, \eta - \frac{\beta_S}{\lambda} \right) * \mathbf{F}_\eta \left[f_d(y_S) \text{rect} \left(\frac{y_S}{d} \right) \right] \frac{1}{d} \sum_{m=-\infty}^{\infty} \delta \left(\eta + \frac{m}{d} \right) \delta(\xi) \right\} ** \pi a^2 \text{somb} \left(2a \sqrt{\xi^2 + \eta^2} \right) \\
&= -\frac{j\gamma A e^{jkr}}{\lambda r} \sum_{m=-\infty}^{\infty} \mathbf{F}_{\frac{m}{d}} \left[f_d(y_S) \frac{1}{d} \text{rect} \left(\frac{y_S}{d} \right) \right] \text{somb} \left(2a \sqrt{\left(\xi - \frac{\alpha_S}{\lambda} \right)^2 + \left(\eta + \frac{m}{d} - \frac{\beta_S}{\lambda} \right)^2} \right) .
\end{aligned} \tag{5.183}$$

Notice that diffraction efficiencies are defined exactly as in the classical case, where Eq. (5.179) is used to find E_m^A . Diffraction orders are evenly spaced on the observation hemisphere. Note that the results above are consistent with the geometric OPD calculation presented in Eqs. (5.168) through (5.173), if the observation is made on the same hemisphere.

A distortion of order position results from observing the diffraction on a plane, rather than a sphere. Figure 5.79 illustrates projection onto the observation hemisphere and the projection onto a flat surface at the vertex of the reference sphere. The diffraction orders are linearly distributed on the observation hemisphere, but they form a curved intercept line on the flat surface. The linearity of the orders on the observation hemisphere leads to important concepts derived in Chapter 9. The diffraction orders are said to be linear in *direction cosine space*.

5.5.3 Resolution and finesse of thin gratings

The concepts of resolution and finesse applied to gratings usually have to do with their application to spectroscopy, where measurement of source power spectra are desired. Minimum detectable wavelength difference, or *chromatic resolution*, is important. Also significant is the maximum wavelength range that can be detected without ambiguity, which is called the *free spectral range* of the grating. The ratio of the free spectral range to the chromatic resolution is a measure of the number of resolvable wavelengths of the system, and the ratio is called the *finesse* of the instrument.

Consider a grating with classical plane-wave illumination, where the source has two wavelengths, λ_1 and $\lambda_2 = \lambda_1 + \Delta\lambda$. Diffraction patterns from each wavelength are independent, because the beat frequency corresponding to $\Delta\lambda$ is well beyond the detectable frequency range of the detector. A portion of the Fraunhofer irradiance pattern is shown in Fig. 5.80, where the two wavelengths are barely resolved. Since the two patterns are independent, the irradiances add to produce the total irradiance on the

detector. Peaks of order m are resolved if they meet some resolution criteria, as discussed in Section 5.4.2. To simplify the development, we chose a resolution criterion where the peaks are resolved if their separation is equal to

$$\rho_{RES} = \frac{\bar{\lambda}z_0}{2a} \quad , \quad (5.184)$$

where $\bar{\lambda}$ is the average wavelength. Since, according to Eq. (5.177) with $\beta_S = 0$, the m^{th} diffraction order is displaced by

$$y_m = -\frac{m\lambda z_0}{d} \quad , \quad (5.185)$$

the physical separation at the limit of detection is

$$\begin{aligned} \frac{\bar{\lambda}z_0}{2a} &= y_m(\lambda_1) - y_m(\lambda_2) \\ &= -\frac{m\lambda_1 z_0}{d} + \frac{m(\lambda_1 + \Delta\lambda) z_0}{d} \quad . \end{aligned} \quad (5.186)$$

With the additional information that $2a = Nd$, where N is the number of illuminated grating lines, Eq. (5.186) reduces to

$$\Delta\lambda_{RES} = \frac{\bar{\lambda}}{mN} \quad , \quad (5.187)$$

where the wavelength difference $\Delta\lambda_{RES}$ is the chromatic resolution of the grating.

The free spectral range of the system is determined at the point where the $m + 1$ order of λ_1 overlaps the m^{th} order of λ_2 . At this point, the irradiance patterns become ambiguous. Mathematically,

$$(m+1)\lambda_1 = m\lambda_2 = m(\lambda_1 + \Delta\lambda_{FSR}) \quad , \quad (5.188)$$

or

$$\Delta\lambda_{FSR} = \frac{\lambda_1}{m} \approx \frac{\bar{\lambda}}{m} \quad , \quad (5.189)$$

because the wavelengths are nearly equal.

The ratio of the free spectral range and the chromatic resolution is the finesse, which is given by

$$\mathcal{F} = \frac{\Delta\lambda_{FSR}}{\Delta\lambda_{RES}} = N \quad . \quad (5.190)$$

This curious result states that the finesse of the spectrometer is increased only by illuminating more grating lines. It is analogous to the result in a Fabry-Perot interferometer, where the finesse is increased only by increasing the reflectivity of the cavity mirrors. In both cases, more resonant modes are used to sharply define the peaks as finesse increases.

5.5.4 Thick gratings and Bragg diffraction

The Q factor, defined by Kogelnik for transmission phase gratings,¹ is often used as an indication of diffraction regimes,² where

$$Q = \frac{2\pi\lambda h}{n_0 d^2 \cos\theta} \quad , \quad (5.191)$$

λ is the vacuum wavelength of an incident plane wave, n_0 is the average refractive index of the grating structure, h is the thickness of the grating, d is the grating period, and θ is the angle of the incident plane wave inside the medium. Q decreases as the thickness decreases and the period increases. In order to analyze diffraction from these elements in terms of a simple transmission function, $Q \ll 1$. Usually, $Q < 0.1$ is sufficient for the “thin” approximation to be valid. For example, a 50% duty cycle square-wave grating made of transparent optical glass with $n_g = 1.5$ in air gives $n_0 = 1.25$. For $d = 10 \mu\text{m}$, $\lambda = 0.5 \mu\text{m}$, $\theta = 0$ and $h = 0.5 \mu\text{m}$ (0.5 waves of OPD between open and glass portions of the grating), $Q \sim 0.01$, which is well into the thin regime. In this case, volume diffraction effects are not severe. A simple transmission function is sufficient to describe physical diffraction. When these conditions are not met, consideration for Bragg diffraction must be made. In addition, it is often the case that rigorous electromagnetic solvers must be used in place of the scalar analysis, as presented in Chapters 20 and 21. Also, metallic gratings often require the use of rigorous electromagnetic solvers due to polarization effects. In this section, scalar Bragg diffraction is presented as an extension to interference principles presented in Chapter 4.

Bragg diffraction was first used to explain x-ray scattering from crystals, for which it gained the inventors the Nobel Prize in 1915. Analysis of scattering from objects with regularly-spaced, multiple-layered structures, like molecular layers in crystals, is diagrammed in Fig. 5.81. The structure consists of regularly spaced xy planes with spacing Λ . An incident plane wave \mathbf{k}_1 illuminates the structure from the left. Each plane reflects or transmits a portion of the wave reaching it, and a portion transmits through it.

¹ H. Kogelnik, “Coupled wave theory for thick volume holograms,” *Bell Syst. Tech. J.*, **48**, 2909-2947 (1969)

² R. Magnusson and T. K. Gaylord, “Diffraction regimes of transmission gratings,” *JOSA*, **68**(6), 809 (1978)

By application of Eq. (4.74) from our study of the Fizeau interferometer, reflection from adjacent planes will produce constructive interference if

$$2n\Lambda \cos \theta = m\lambda \quad , \quad (5.192)$$

where n is the refractive index in the medium, θ is the angle of incidence in the medium and λ is the vacuum wavelength. If each pair of adjacent planes reflects light in phase according to Eq. (5.192), the total amount of reflected light can be very intense. With a sufficient number of layers and low absorption, the reflection can be nearly complete, with essentially no transmitted wave. With $m = 1$, Eq. (5.192) is simply a statement of Bragg's Law.

More generally, Eq. (5.192) can be rewritten as a vector equation with

$$\mathbf{k}_1 - \mathbf{k}_2 = \mathbf{g} \quad , \quad (5.193)$$

where \mathbf{k}_2 is the diffracted wave and \mathbf{g} is the grating vector defined with $\hat{\mathbf{g}}$ perpendicular to the structure planes and

$$\mathbf{g} = \frac{2\pi}{\Lambda} \hat{\mathbf{g}} \quad . \quad (5.194)$$

It is no accident that Eqs. (5.193) and (5.194) bear a striking resemblance to our discussion of two-plane-wave interference in Section 4.1.1.2. The analogy is perfect, with fringe planes replaced by structure planes and $\mathbf{k}_\Delta = \mathbf{g}$. These relationships are often depicted in vector diagrams, like those shown in Fig. (5.82) for a reflecting and transmitting structures.

Given the analogy with two-plane wave interference, one can conceptualize formation of structure planes in photosensitive material with simple two-beam interferometric setups. This basic concept is the basis of volume holography, where materials like dichromated gelatin are used to form volume phase holograms that work according to Bragg diffraction. Beyond simple two-beam plane-wave interference, spherical wave interference is used to form volume phase structures that efficiently produce true reconstruction of three-dimensional objects. Microscopic inspection of the volume structures indicate that they behave locally like the structure shown in Fig. 5.81.

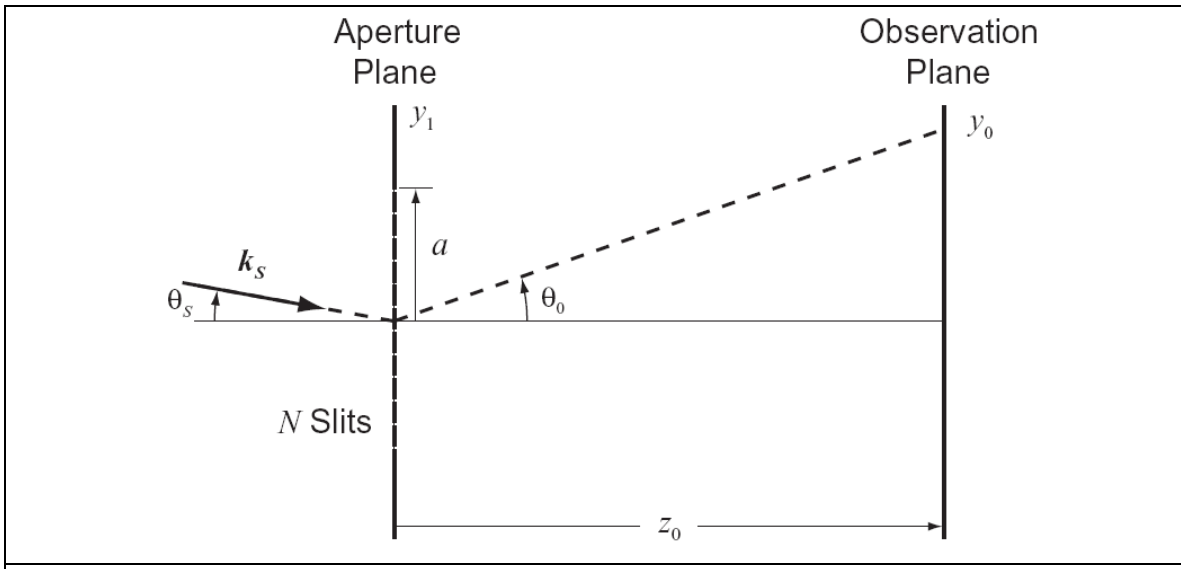


Figure 5.72 Grating with classical plane-wave illumination.

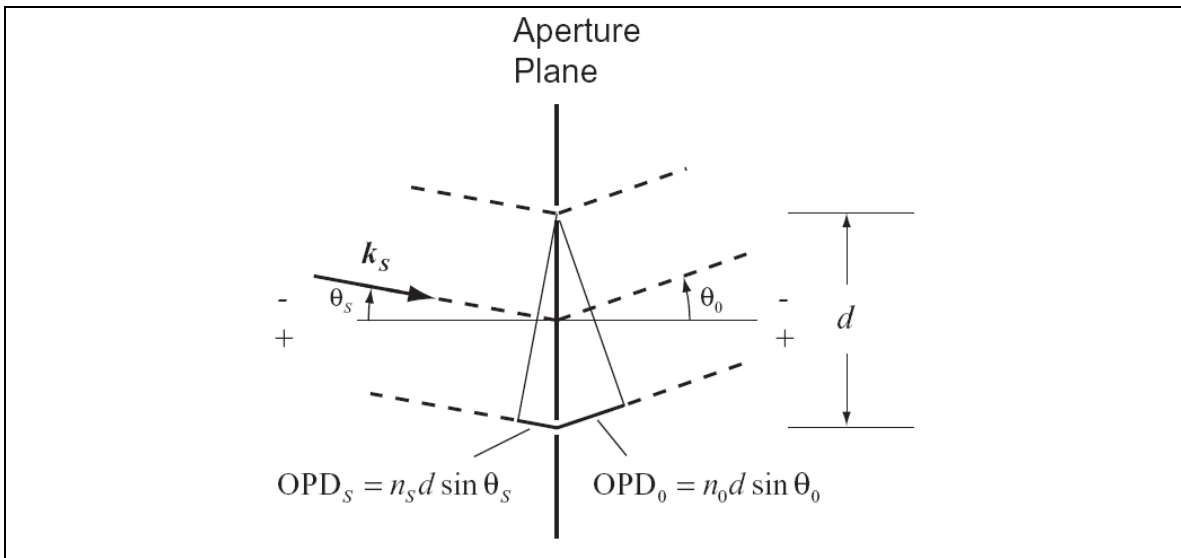


Figure 5.73. Grating slit pair with classical plane-wave illumination.

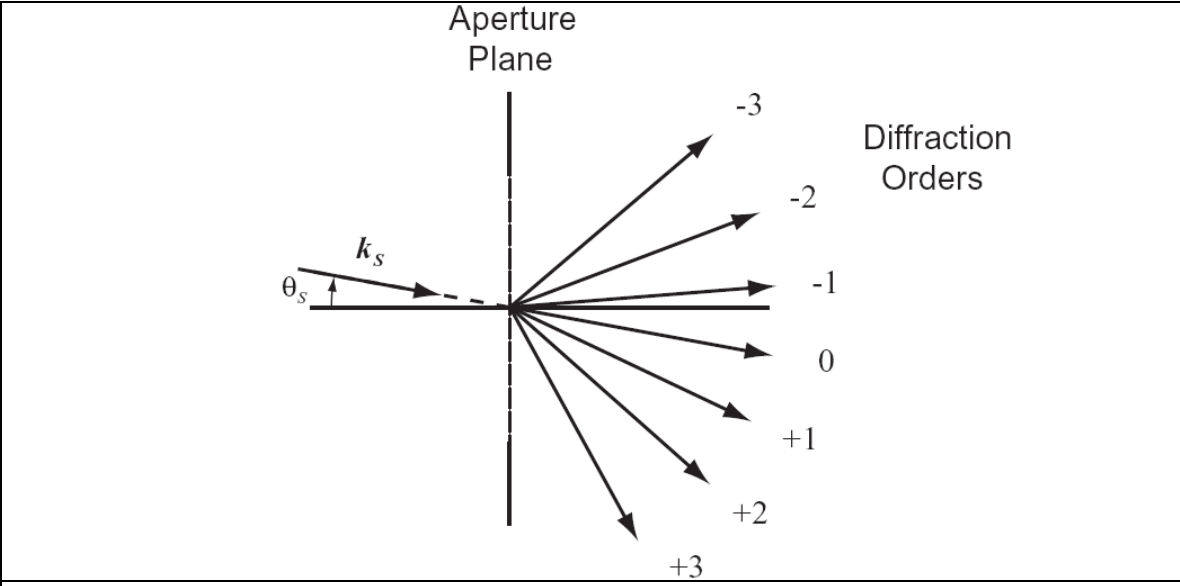
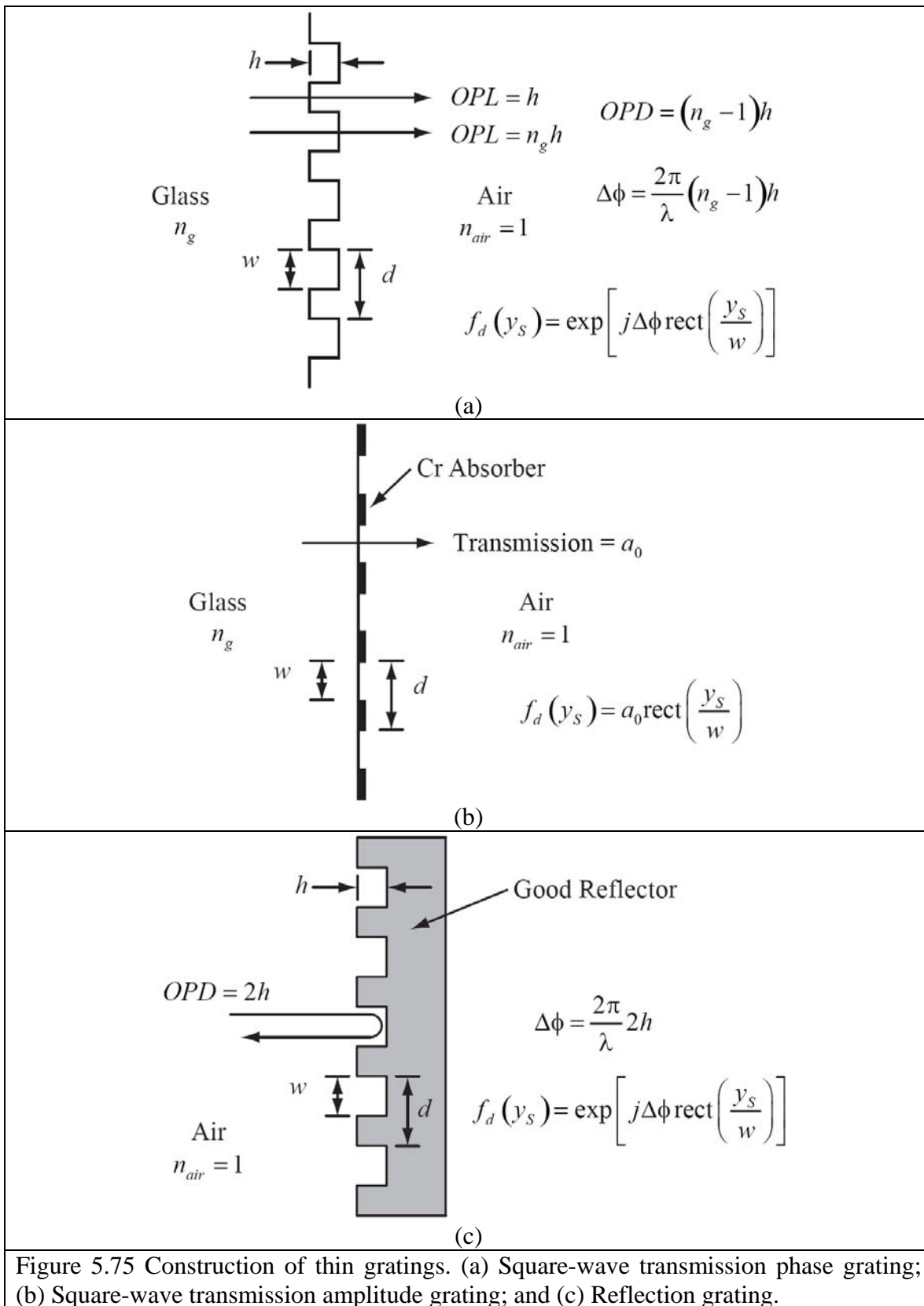


Figure 5.74. Diffraction orders for a grating with classical plane-wave illumination.



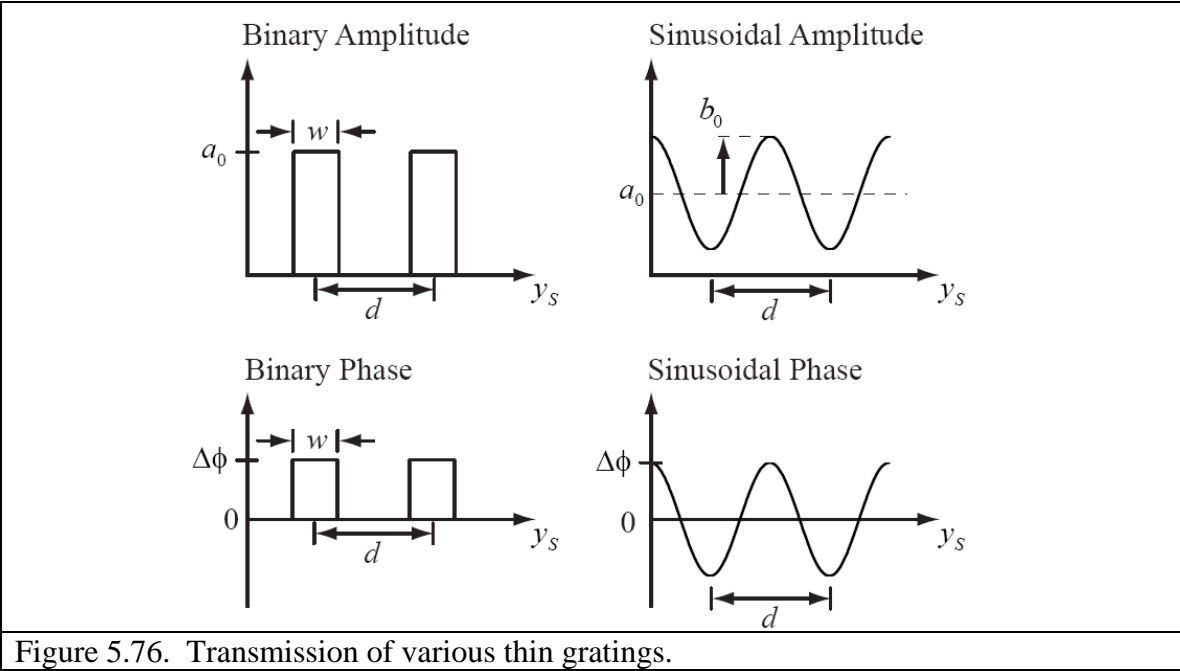


Figure 5.76. Transmission of various thin gratings.

Grating Type	$f_d(y_s)$	Absolute Diffraction Efficiency (E_m^A)	$(E_{\pm 1}^A)_{\max}$
Binary Amplitude	$a_0 \text{rect}\left(\frac{y_s}{w}\right)$	$\left(\frac{a_0 w}{d}\right)^2 \text{sinc}^2\left(\frac{wm}{d}\right)$	$\left(\frac{1}{\pi}\right)^2$ if $a_0 = 1$ and $w/d = 0.5$
Sinusoidal Amplitude	$a_0 + b_0 \sin(2\pi y_s / d)$	$\left a_0 \text{sinc}(m) + b_0 \frac{\text{sinc}(m-1) - \text{sinc}(m+1)}{2j} \right ^2$	$\frac{1}{16}$ if $a_0 = b_0 = 0.5$ and $w/d = 0.5$
Binary Phase	$\exp\left[j\phi_0 \text{rect}\left(\frac{y_s}{w}\right) \right]$	$\left(\frac{w}{d}\right)^2 \text{sinc}^2\left(\frac{wm}{d}\right) + \left(1 - \frac{w}{d}\right)^2 \text{sinc}^2\left[\frac{m}{2}\left(1 - \frac{w}{d}\right)\right] \cos^2\left[\frac{\pi m}{2}\left(1 + \frac{w}{d}\right)\right] + 2\left(\frac{w}{d}\right)\left(1 - \frac{w}{d}\right) \text{sinc}\left(\frac{wm}{d}\right) \text{sinc}\left[\frac{m}{2}\left(1 - \frac{w}{d}\right)\right] \times \cos\left[\frac{\pi m}{2}\left(1 + \frac{w}{d}\right)\right] \cos\phi_0$	$\left(\frac{2}{\pi}\right)^2$ if $\phi_0 = \pi$ and $w/d = 0.5$
Sinusoidal Phase	$\exp\left[j\phi_0 \cos(2\pi y_s / d) \right]$	$ J_m(\phi_0) ^2$	0.34 if $\phi_0/2\pi = 0.293$ (See Fig. 5.78)

Figure 5.77. Diffraction efficiencies of various thin gratings.

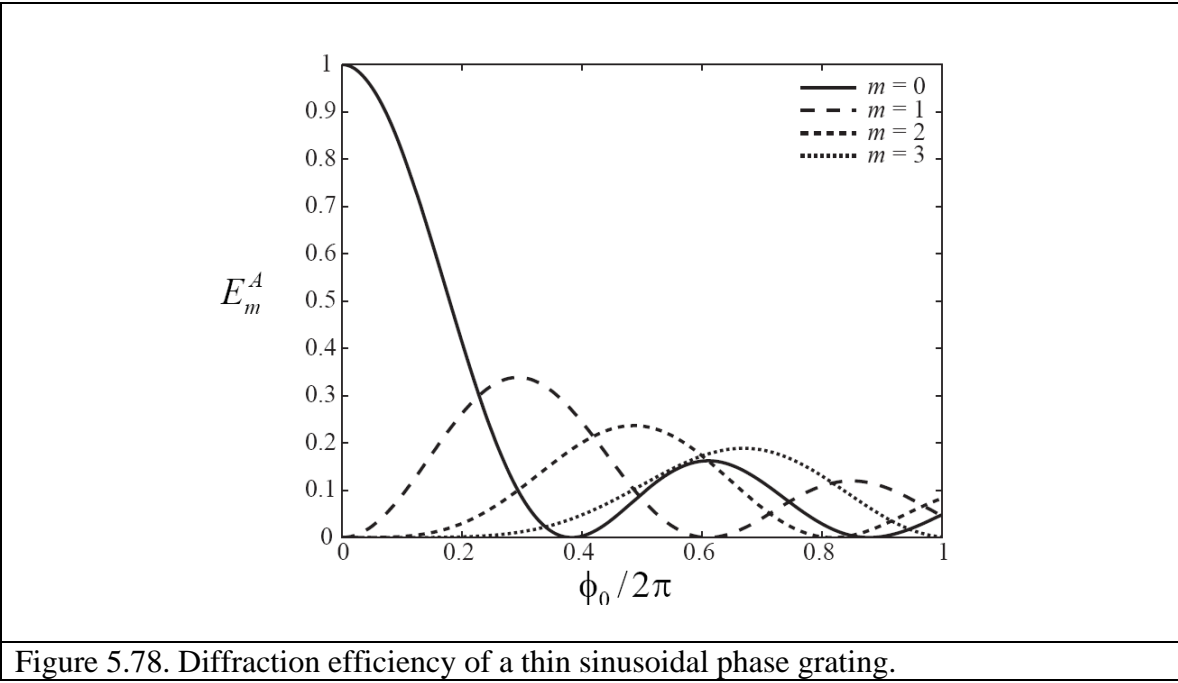


Figure 5.78. Diffraction efficiency of a thin sinusoidal phase grating.

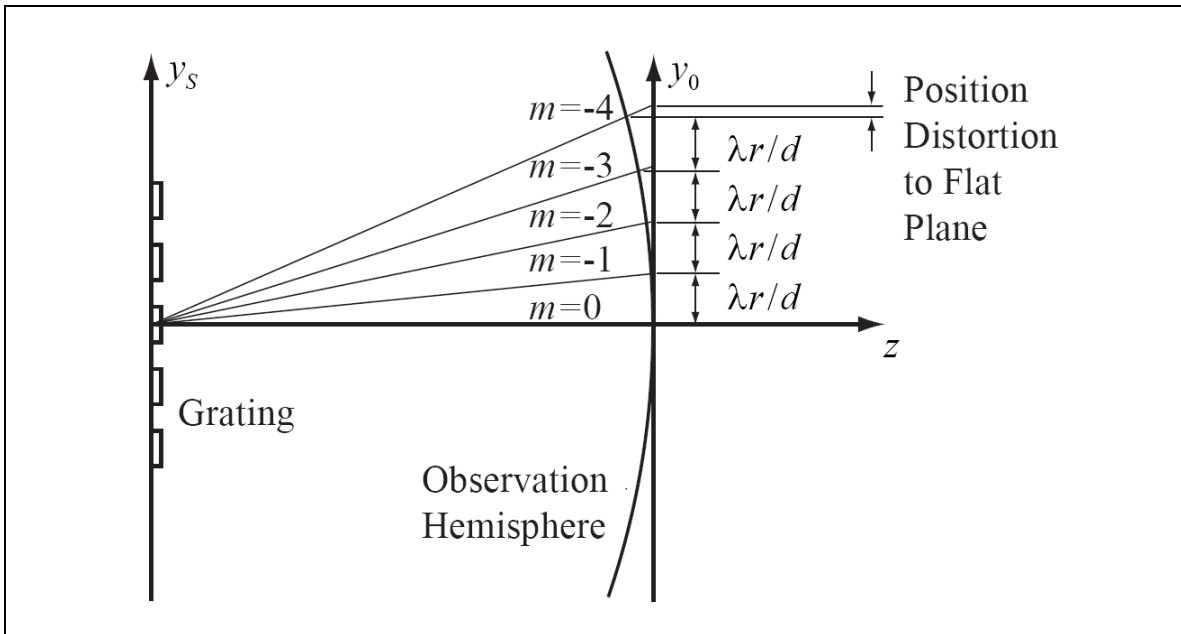


Figure 5.79. Large angle diffraction from a thin phase grating. Diffraction orders are evenly spaced by $\lambda r/d$ on the observation hemisphere, but projection to a plane introduces distortion.

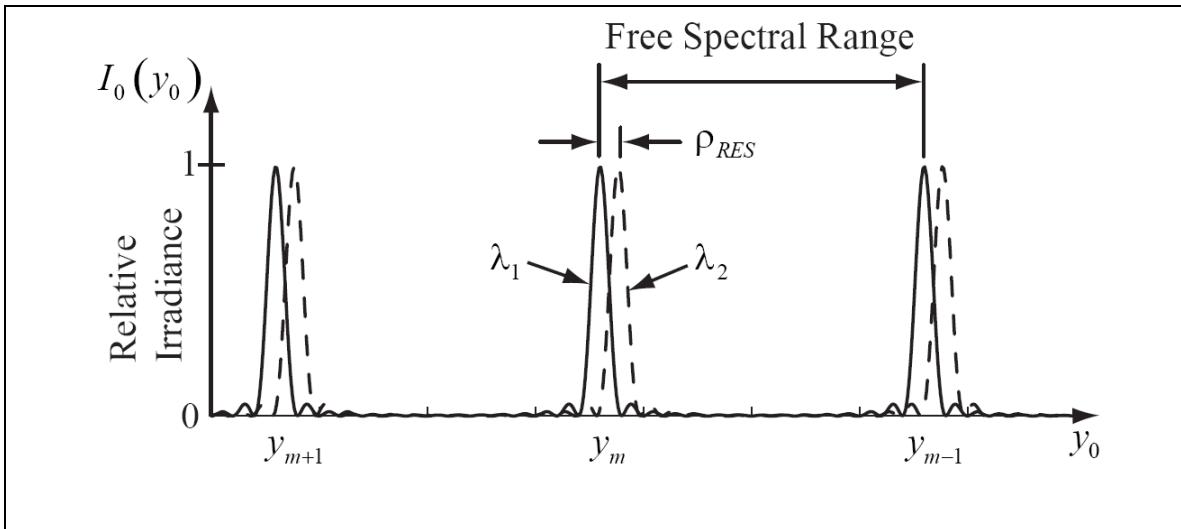


Figure 5.80. Diffracted orders from a grating with a two-wavelength source.

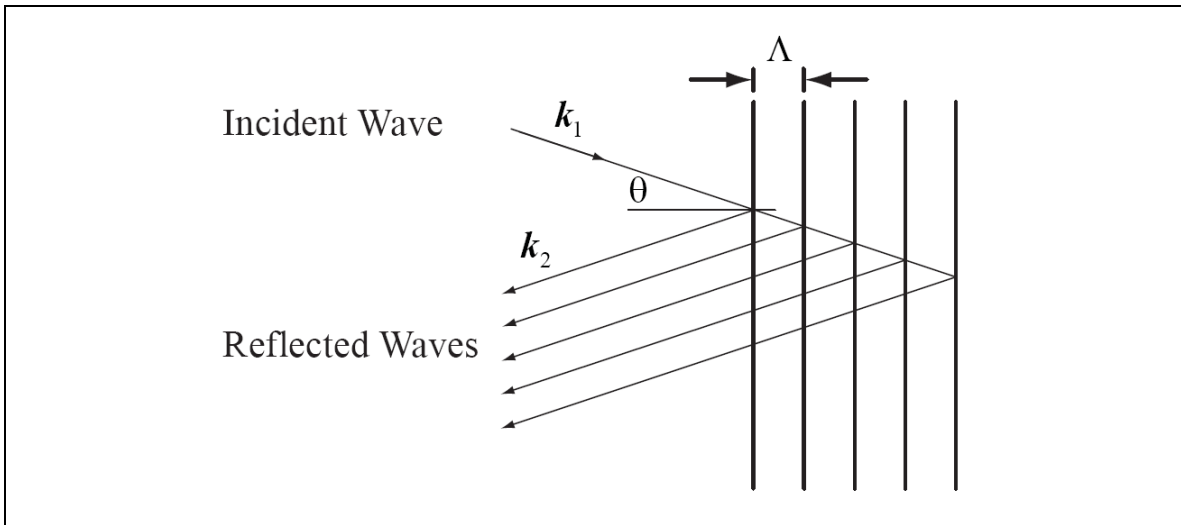


Figure 5.81. Bragg diffraction from a multiple-layered structure.

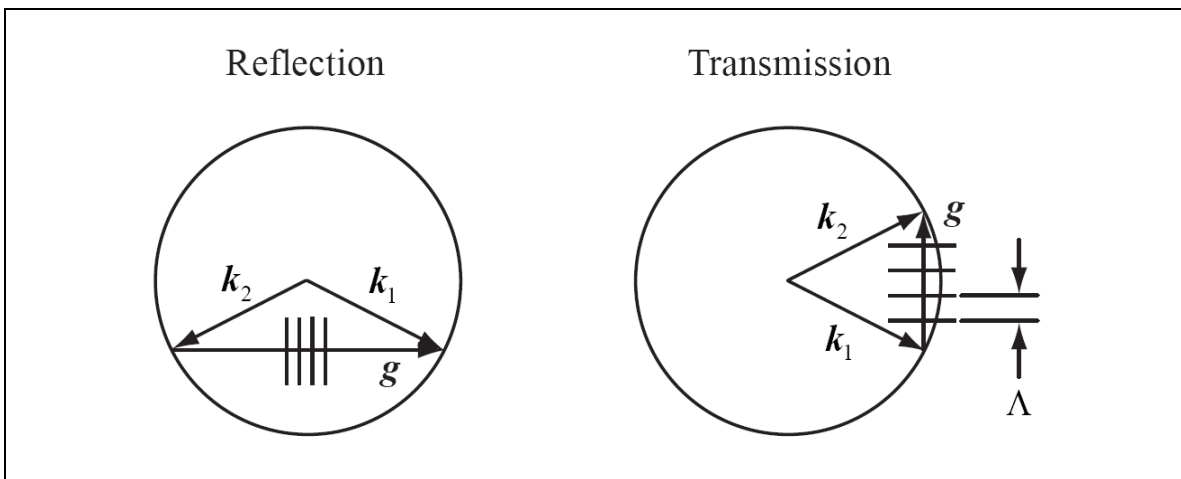


Figure 5.82. Vector diagrams for Bragg diffraction in reflection and transmission